Liquid Crystals
Publication details, including instructions for authors and subscription information:
http://www.tandfonline.com/loi/tlct20

Low and high frequency dielectric spectroscopy on a liquid crystal with the phase sequence N*-S_A-S*$_C$

M. R. De La Fuente [a] , M. A. Pérez Jubindo [a] , J. Zubia [b] , T. Pérez Iglesias [c] & A. Seoane [d]

[a] Departamento de Física Aplicada II, Facultad de Ciencias, Universidad del Pais Vasco, Apdo. 644, 48080, Bilbao, Spain

[b] Departamento de Automática, Electrónica y Telecomunicaciones, E.T.S.I.I.T., Universidad del País Vasco, Alameda de Urquijo s/n, 48013, Bilbao, Spain

[c] Departamento de Física Aplicada, Facultad de Ciencias, Universidad de Vigo, Vigo, Spain

[d] Departamento de Teoría de la Señal, E.T.S.I.T., Universidad de Vigo, Vigo, Spain

Version of record first published: 24 Sep 2006.

To cite this article: M. R. De La Fuente , M. A. Pérez Jubindo , J. Zubia , T. Pérez Iglesias & A. Seoane (1994): Low and high frequency dielectric spectroscopy on a liquid crystal with the phase sequence N*-S_A-S*$_C$, Liquid Crystals, 16:6, 1051-1063

To link to this article: http://dx.doi.org/10.1080/02678299408027874

LIQUID CRYSTALS, 1994, VOL. 16, NO. 6, 1051–1063

Low and high frequency dielectric spectroscopy on a liquid crystal with the phase sequence N^*–S_A–S_C^*

by M. R. DE LA FUENTE*†, M. A. PÉREZ JUBINDO†, J. ZUBIA‡, T. PÉREZ IGLESIAS§ and A. SEOANE¶

† Departamento de Física Aplicada II, Facultad de Ciencias, Universidad del País Vasco, Apdo. 644, 48080 Bilbao, Spain
‡ Departamento de Automática, Electrónica y Telecomunicaciones, E.T.S.I.I.T., Universidad del País Vasco, Alameda de Urquijo s/n, 48013, Bilbao, Spain
§ Departamento de Física Aplicada, Facultad de Ciencias, Universidad de Vigo, Vigo, Spain
¶ Departamento de Teoría de la Señal, E.T.S.I.T., Universidad de Vigo, Vigo, Spain

(*Received 1 June 1993; accepted 8 October 1993*)

Broadband dielectric measurements on a multicomponent ferroelectric liquid crystal mixture have been performed. The alignment was homeotropic and the cell and sample holder were the same in the whole frequency range. Two relaxation processes have been observed in all liquid crystal phases with shapes given by the Havriliak–Negami and inverted Havriliak–Negami functions. Strengths and frequencies of both modes have been obtained for the different phases. The values of the latter and their activation energies allowed us to assign the low and high frequency mechanism to the molecular reorientation around the transversal axis and around the longitudinal axis, respectively. The behaviour of this high frequency mode does not show any jump in the S_A–S_C^* phase transition, neither in the amplitude nor in the frequency, indicating that the appearance of the spontaneous polarization in the S_C^* phase is not the consequence of the freezing of this mode.

1. Introduction

Dielectric spectroscopy of ferroelectric liquid crystals (FLC) has been commanding increasing interest in the past few years. In the frequency regime from DC to some GHz, it delivers not only the collective modes directly associated with the ferroelectricity (soft mode and Goldstone mode), but also the molecular modes. These have been studied very extensively in the past, but above all for nematic phases, for which microscopic and statistical theories also exist and account for the observed behaviour [1–8]. These molecular modes have not been so extensively studied for FLC, due probably to the interest of most authors in the planar alignment, where all the specific characteristics of these mesophases appear [9–11], and which is also the alignment required for most of their electro-optical applications. In this geometry, the strengths of the soft and Goldstone modes can hide their contribution to the dielectric response. However, the dynamics of these modes have much to say about the microscopic origin of ferroelectricity in liquid crystals.

Experimentalists must face several problems in order to perform broadband dielectric studies of these materials. First of all, the use of different apparatus is needed to cover the required spectrum. Furthermore, the sample holder most adequate in a

* Author for correspondence.

0267-8292/94 $10·00

given case might not be the same in another, and then similar experimental conditions are not guaranteed. This problem is important for the GHz frequency range, if you have a small amount of substance and you have to align it using high conductivity electrodes.

Recently some discussion has appeared in the literature related to whether the dielectric relaxation observed at a few GHz in homogeneously aligned samples in the ferroelectric phase is related to the two polarization modes predicted by the generalized mean field theory [12, 13]. A recent paper [14] showed that the fact that one can only observe one relaxation process is due to the small splitting of the two high frequency modes on going from the paraelectric S_A phase to the ferroelectric S_C^* phase. Hence, it was proposed that a revision of the theory, in the sense proposed in references [15, 16], is not needed. If this is so, the experimental behaviour of both amplitude and frequency are very far from theoretical predictions [17–19]. Besides, the usual explanation of the origin of ferroelectricity in liquid crystals is not in accordance with experimental results. Some authors point to a free rotation about the molecular long axes which becomes hindered on going from the S_A phase to the S_C^* phase and also slows down with freezing of the mode [20], with the appearance of a spontaneous polarization in each smectic layer. Nevertheless, most experimental work does not indicate such a drastic change on going from the paraelectric to the ferroelectric phase neither in the amplitude nor the frequency, indicating that the mechanism responsible does not change basically [17–19]. These studies seem to be in better accordance with the microscopic model of Urbanc and Zeks [21, 22] which assumes that the order of the transverse dipoles is induced only by the tilt via a chiral and a non-chiral contribution to the potential seen by the dipoles. In this model the spontaneous polarization is related to the asymmetry introduced by the non-chiral term. Then, the rotation around the molecular long axis could be considered as a hindered rotation in both the paraelectric and ferroelectric phases, but with an asymmetry in the latter.

In order to contribute to the clarification of these points, we have performed a dielectric study on a room temperature ferroelectric liquid crystal—the mixture SCE9 from Merck Ltd, U.K. It has the phase sequence I–N*–S_A–S_C^*–C. Amplitudes, frequencies and activation energies of the different modes in all the mesophases, with homeotropic alignment, have been determined from the dielectric response in the frequency range 100 Hz to 1 GHz.

2. Experimental

The dielectric study was performed mainly using cells with metallic electrodes. Although the use of ITO coated glass plates allows a simultaneous optical control of the alignment, the relaxation associated with the high resistance value of this type of electrode could mask some of the contributions.

Complex dielectric permittivity has been measured with two different impedance analysers—the HP4191A for the 10^6–10^9 Hz range and the HP4192A for the 10^2–10^6 Hz range. The former measures the impedance of the sample from the reflection coefficient at the end of a 50 Ω coaxial transmission line. In order to guarantee the same alignment conditions over the whole frequency range, the same cell must be used for both frequency ranges. Thus, the cell consists of two gold plated brass electrodes (diameter 3 mm) separated by two 50 μm thick silica spacers, making a plane capacitor located at the end of the line. We used as sample holder a modified HP16091A coaxial test fixture. This was adapted by a connector which allows us to go from APC7 to four wires, with a residual capacity of 2·5 pF, in order to perform

measurements with the low frequency analyser. The sample holder was held in a cryostat, which screens the system, and both temperature and dielectric measurements were fully computer controlled.

Once the specimen was in the cell, it was heated into the isotropic phase and then slowly cooled down to give the different mesophases. We did not apply any magnetic field and did not treat the metallic surfaces. The permittivity did not show an increase in the S_C^* phase, which, in view of the large value of the Goldstone mode strength in the planar alignment, allowed us to be sure that the alignment was homeotropic. Nevertheless, in order to confirm this point, we made a transparent cell with ITO coated electrodes. The glass plates were treated with HTAB in order to obtain the homeotropic alignment. The cell thickness was also 50 μm. With these cells, we measured the dielectric permittivity in the 10^2–10^6 Hz range and, after subtracting the cell relaxation, we found exactly the same dielectic behaviour as with the other cells. In this compound the cholesteric pitch is very large near the S_A phase which causes the cholesteric helix to become unwound, and then the homeotropic alignment is obtained both in the N* and in the S_A phase. Optical observation allowed us to confirm that in the S_A phase the homeotropic alignment was perfect.

3. Results and discussion

As we have above mentioned the compound under study is a multicomponent mixture from Merck Ltd, U.K. It shows the phase sequence

$$S_C^*\text{–}(56^\circ)\text{–}S_A\text{–}(90{\cdot}7^\circ C)\text{–}N^*\text{–}(119^\circ C)\text{–}I$$

The transition temperatures have been deduced from texture changes seen using the polarizing microscope and are in accordance with the results of the dielectric study. This compound has been the subject of several studies in our laboratory [23, 24]. The transition temperatures were found to be somewhat different from those published [23, 24]. The reason for this discrepancy may be related to the period of time that elapsed between these sets of measurements, during which some degradation of the material could have occurred. In particular, we note that the maximum strength of the Goldstone mode was about 160, the spontaneous polarizarion had a value of 15 nC cm^{-2} and the tilt was 25 deg at 10°C below the S_A–S_C^* phase transition.

Before discussing our results, we shall describe some molecular and geometric parameters (see figures 1 and 2). Although the system is a mixture, we observe relaxations that can be explained as due to one type of molecule. Then, we will consider 'mean' molecules with a dipole moment $\boldsymbol{\mu} = \boldsymbol{\mu}_l + \boldsymbol{\mu}_t$, where μ_l stands for the component of the dipole moment along the molecular long axis and μ_t for the transverse component. In the S_A and the unwound N* phases, the instantaneous molecular director makes an angle θ with the applied electric field, which is normal to the smectic layers. We will assume that in the S_C^* phase, the smectic layers remain parallel to the electrodes with the helix axis parallel to the electric field.

Figure 3 shows the temperature dependence of the *static* homeotropic dielectric permittivity. We shall explain below how we obtained it. One can see a clear decrease when going from the N* to the S_A^* phase, which is mainly due to the decrease of the contribution related to the component of the dipole moment in the transverse direction to the molecular long axis (μ_t). Moreover, an increase can be seen when going from the S_A to the S_C^* phase, which is due to the increase of the contribution related to the longitudinal component of the dipole moment (μ_l), as we shall show below. A positive slope in ε_s, in the homeotropic alignment, versus $T$is usually explained in terms of an

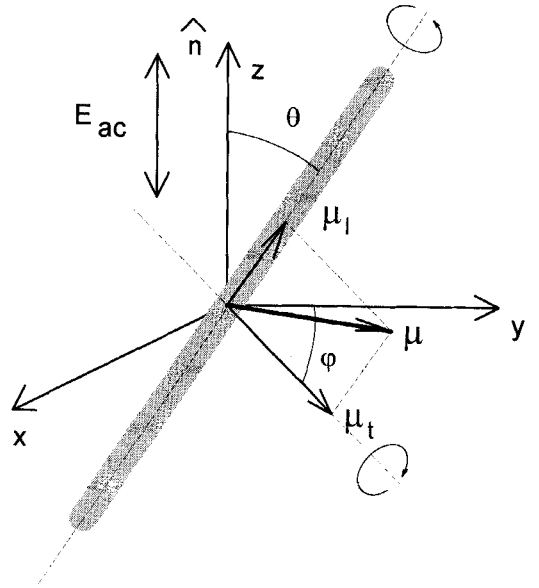

Figure 1. S_A and unwound N* coordinate geometry.

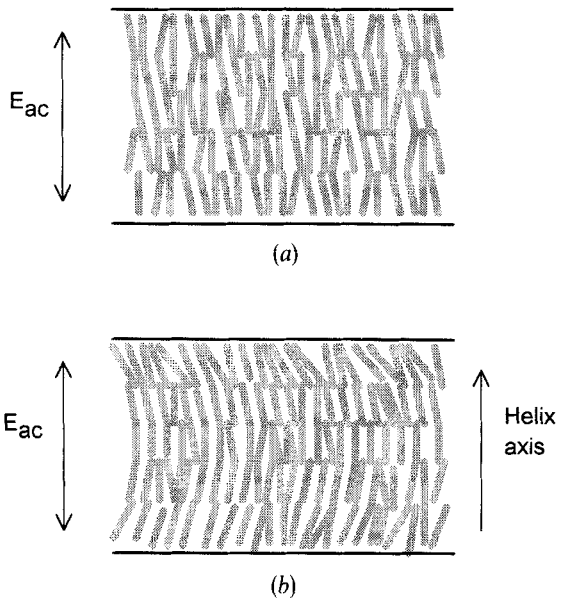

Figure 2. (*a*) Measurement geometry in the S_A phase. (*b*) Measurement geometry in the S_C^* phase.

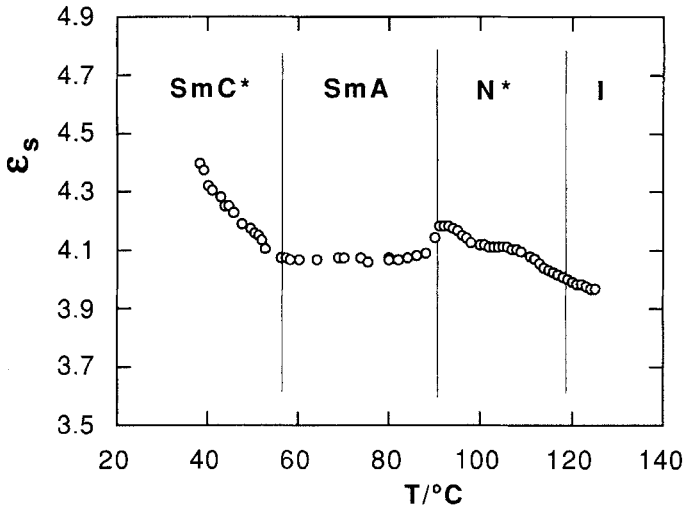

Figure 3. Temperature dependence of the static homeotropic permittivity.

antiparallel correlation between the dipole moments along the molecular long axis [25, 26], but this is not the case here because, as we shall show later, it is related to the dipole moment in the transverse direction.

When performing a frequency scan, dielectric spectroscopy is able to distinguish among possible molecular motions, whenever they can be coupled with the electric field, and to separate their contributions to the dielectric permittivity, because of their different characteristic frequencies and, in general, important dipole moments. With this aim, the complex permittivity was measured between 10^2 and 10^9 Hz for all phases. The measurements show that two different separated relaxations with different strength, frequency and temperature behaviour are present from the isotropic to the S_C^* phase. Figure 4(*a*) shows a typical plot of the imaginary part of the complex permittivity (losses) ε'' versus the logarithm of the frequency, for a temperature in the S_C^* phase. Figure 4(*b*) shows the real part, ε', for the same temperature. In figure 5 we have represented the corresponding Cole–Cole plot, ε'' versus ε' (the results for the S_A phase are similar). Unfortunately the small geometric capacity of the capacitor used did not allow us to obtain the losses below 10^4 Hz. The results were fitted to

$$\varepsilon(\omega) = \Delta\varepsilon_l(\omega) + \Delta\varepsilon_t(\omega) + \varepsilon_\infty, \tag{1}$$

where $\Delta\varepsilon_l(\omega)$ stands for the contribution due to the mechanism relaxing on the low frequency side of the scanned spectrum, $\Delta\varepsilon_t(\omega)$ for the high frequency one and ε_∞ for the residual high frequency permittivity after the relaxation of both.

The low frequency relaxation was fitted in both smectic phases to the inverted Havriliak–Negami equation [27]

$$\Delta\varepsilon_l(\omega) = \Delta\varepsilon_l\left[1 - \left\{\frac{(i\omega\tau)^{1-\alpha}}{1+(i\omega\tau)^{1-\alpha}}\right\}^{\beta}\right], \tag{2}$$

with $\alpha = 0{\cdot}12$ and $\beta = 0{\cdot}9$ almost generally. It is worth pointing out that the results could also be fitted to the normal Havriliak–Negami equation (see equation (3) below), but with $\beta > 1$ [28]. $\Delta\varepsilon_l$ stands for the strength of this contribution. Its frequency for maximum losses is about 30 MHz in the isotropic phase and about 30 kHz in the S_C^*

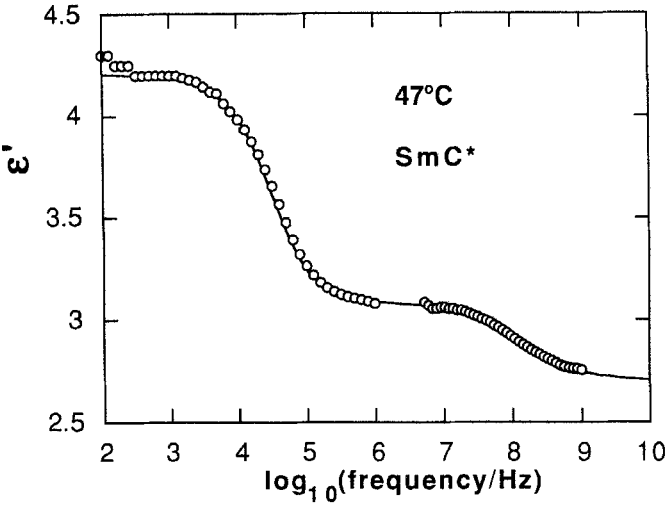

(*a*)

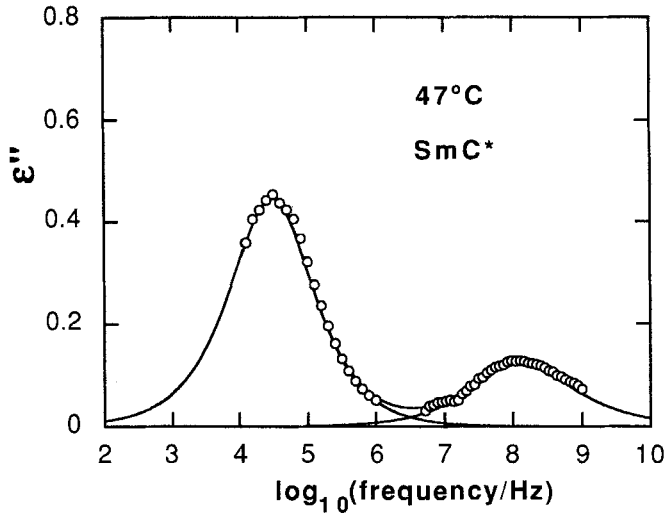

(*b*)

Figure 4. Dots—frequency dependence of the dielectric losses (*a*) and of the real part of the permittivity (*b*) in the S_C^* phase. The sample was aligned with the helix axis perpendicular to the electrodes. The low frequency relaxation is related to the longitudinal dipole moment and the high frequency relaxation to the transverse dipole moment. Continuous line: fitting to equations (2) and (3).

phase. These values, accounting for a high thermal activation, allowed us to assign it to the reorientation of the molecular long axis [6, 29–31]. This strong thermal activation is due to the hindrance of this rotation when the longitudinal dipole has to rotate in the nematic or smectic potential.

The high frequency relaxation was fitted to the Havriliak–Negami equation

$$\Delta\varepsilon_t(\omega) = \Delta\varepsilon_t \left\{ \frac{1}{\{1+(i\omega\tau)^\alpha\}^\beta} \right\}, \tag{3}$$

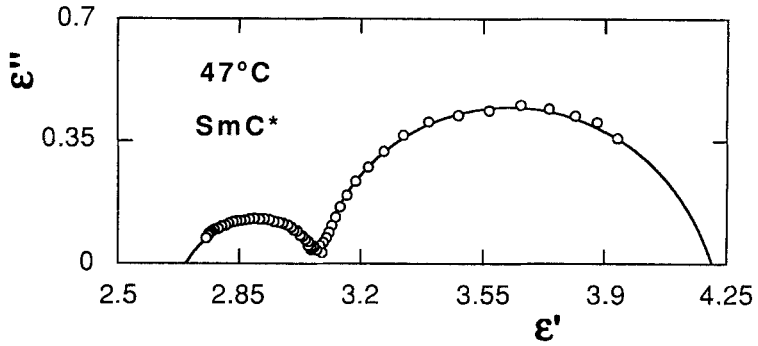

Figure 5. Cole–Cole plot, ε'' versus ε'. Same conditions as figure 4.

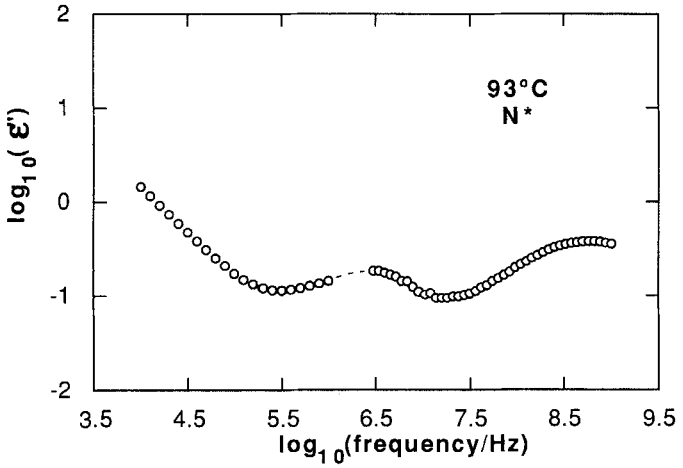

Figure 6. Log–log plot of ε'' versus frequency in the N* phase. Low frequency losses show a high DC conductivity contribution.

with α ranging from 0·1 to 0·2 and β from 0·75 to 0·9 almost generally. The frequency of the maximum losses of this mechanism, f_1 obtained from the parameters of the fitting through

$$f_1 = \frac{1}{2\pi\tau}\left\{\tan\left(\frac{\pi}{2(\beta+1)}\right)\right\}^{1/\alpha} \tag{4}$$

is about 10^9 Hz in the isotropic phase and shows a smaller thermal activation than the other relaxation. It is related to the rotation around the molecular long axis and so to the transverse dipole moment [6, 18, 26, 30].

Figures 6 and 7 show the losses versus frequency (log–log plot) in the N* and I phases, respectively. In both phases, an important DC conductivity contribution to the losses can be observed. The fact that in the isotropic phase two different relaxations occur allows us to consider two independent motions for the molecule. On the other hand, the strength of the high frequency contribution is larger than that of the low frequency one, and so we can assume that the transverse dipole moment is larger than the longitudinal one, as was expected for a material with a noticeable spontaneous polarization in the ferroelectric phase.

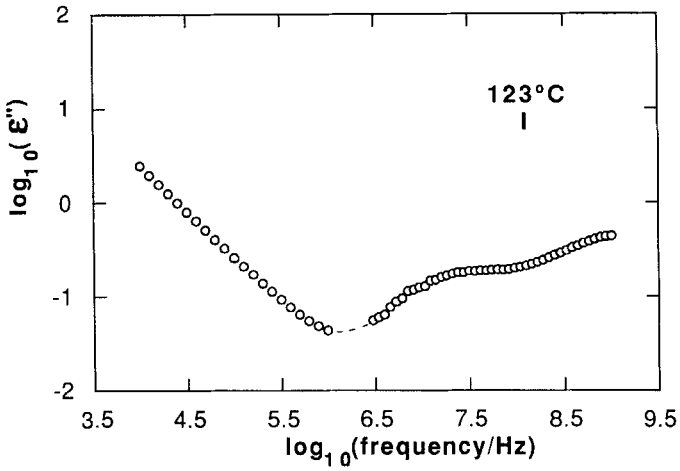

Figure 7. Log–log plot of ε'' versus frequency in the isotropic phase. Low frequency losses show a high DC conductivity contribution.

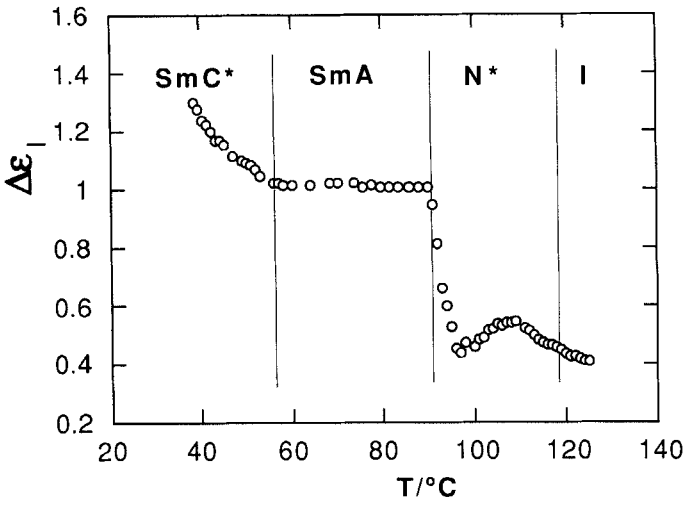

Figure 8. Temperature dependence of the dielectric strength of the low frequency mode. These amplitudes have been deducted from the fittings of the complex permittivity to equations (2) and (3).

From the fittings of the complex permittivity to equations (1) and (2) (lines in figures 4 and 5), we deduced $\Delta\varepsilon_l$ and $\Delta\varepsilon_t$, which are represented in figures 6 and 7, respectively. Unfortunately, the high DC conductivity in the N* and isotropic phases, more marked for the homeotropic alignment, coupled with its small dielectric strength, did not allow us to perform a fitting of the relaxation related to the rotation around the molecular short axis. The strength in these phases was deduced by subtracting from the measured permittivity at 1 kHz (well below its characteristic frequency) $\Delta\varepsilon_t + \varepsilon_\infty$ for each temperature. If the order parameter of the longitudinal axis in the orthogonal S_A phase were unity, no contribution associated with μ_t could be seen (see figures 1 and 2). Therefore, its appreciable value could be related to a high disorder of this phase, a fact frequently found in mixtures [32].

In figure 8 the evolution of $\Delta\varepsilon_t$ as a temperature function can be seen. It shows a general increase when the temperature decreases. The transition from the isotropic to the N* phase cannot be seen in this property. However, when the S_A phase is approached, the behaviour in N* changes. This change coincides with a texture change seen under the polarizing microscope, when the cholesteric pitch becomes longer and longer, and the helix is fully unwound. This strength in the S_A phase is almost constant and in the S_C^* phase shows an increase. This behaviour, which is not due to the tilt, because in any case it should work in the contrary sense, is not the usual one indicating a parallel correlation among longitudinal dipoles [25].

In figure 9, the temperature dependence of $\Delta\varepsilon_t$ can be seen. It shows a strong decrease on going from the N* phase to the S_A phase, which is the result of the ordering of the molecules in layers in an orthogonal mesophase. This tendency is inverted in the S_C^* phase, where the slope of $\Delta\varepsilon_t$ versus T is negative, which is the result of the tilt and of a parallel correlation among tranverse dipole moments as expected for a ferroelectric phase [33].

In figure 10 we have represented the residual high frequency permittivity, ε_∞, as temperature function. There one can see that all through the smectic phases, this is constant and also all through the nematic and isotropic phases, with a jump between the N* phase and the S_A phase. In the isotropic phase, and assuming that the molecule is rod-like (for this high frequency limit)

$$\varepsilon_\infty = \tfrac{1}{3}\varepsilon_{\parallel\infty} + \tfrac{2}{3}\varepsilon_{\perp\infty} = 2{\cdot}5. \tag{5}$$

In the S_A phase and assuming that all molecules are perpendicular to the electrodes

$$\varepsilon_\infty = \varepsilon_{\parallel\infty} = 2{\cdot}7. \tag{6}$$

From the above values, it is obvious that both quantities are temperature independent and $\varepsilon_{\parallel\infty} = 2{\cdot}7$ and $\varepsilon_{\perp\infty} = 2{\cdot}4$. This behaviour, together with its low value (very near n^2) allows us to assign it to the coupling of the electric field with the induced polarization.

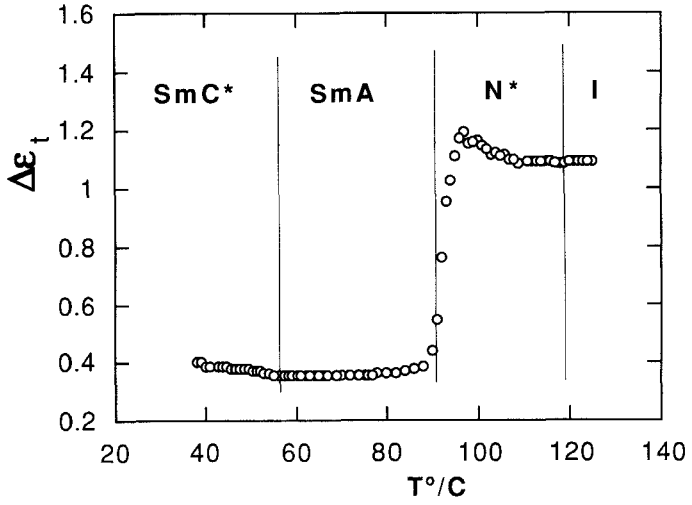

Figure 9. Temperature dependence of the dielectric strength of the high frequency mode. These amplitudes have been deduced from the fittings of the complex permittivity to equations (2) and (3).

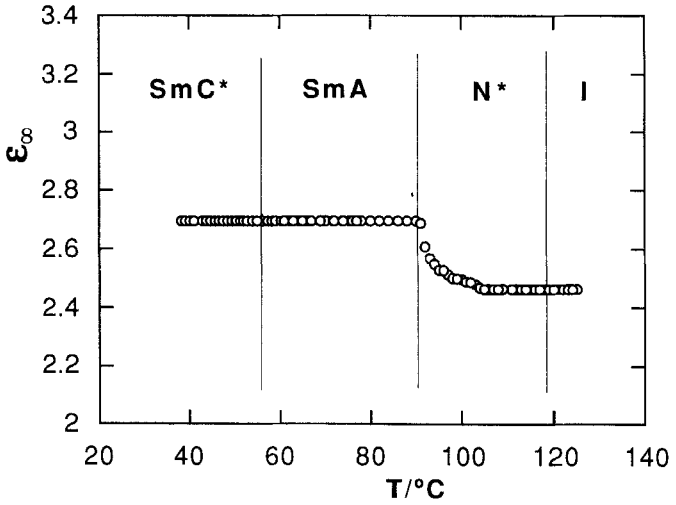

Figure 10. Temperature dependence of the high frequency permittivity in the homeotropic alignment.

Taking into account that measurements have been performed for the homeotropic alignment, this behaviour accounts for the positive anisotropy of the high frequency polarizability, as expected for elongated molecules.

In figures 11 and 12 we have represented the frequency of the maximum losses for the low and high frequency processes versus temperature (Arrhenius plot), respectively. These frequencies have been deduced from the relaxation times of the fittings. We have represented frequency instead of relaxation time, because this depends more on the other parameters of the fitting (α, β) than the frequency does. It is also important to point out that some of the fittings were not easy to perform, because the high frequency relaxation is not well defined.

These frequencies, in all cases have been fitted to the Arrhenius law:

$$f = f_0 \exp(-E_a/kT). \tag{7}$$

For the reorientation of μ_t the activation energy is 81 kJ mol^{-1} in the S_A phase and 103 kJ mol^{-1} in the S_C^* phase. This difference could be due to a stronger hindrance of the reorientation in the smectic potential when the phase is tilted. If one assumes that the molecule rotates as a whole, this relaxation could be described as a rotational diffusion in the smectic potential, and a change in the activation energy could be related to a change in the rotational viscosity for this molecular motion [2, 34]. Unfortunately we do not know the molecular structure of our compound, and so we cannot choose between this model or the flip–flop model for this contribution.

The activation energy for the rotation of μ_t was obtained for all mesophases—36 kJ mol^{-1} in the S_C^*, 29 kJ mol^{-1} in the S_A and 32 kJ mol^{-1} in the N*. The motion around the molecular long axis appears to be very similar in all phases. The usual assumption of free rotation about the long axis in non-ferroelectric phases is not justified. A recent EPR study [35] for a paramagnetic LC with the phase sequence I–S_A–S_C shows that this motion could be described as a libration in a narrow potential well, which expands as the temperature rises. In spite of our lack of knowledge of the main contributions to the transverse dipole moment, taking into account that the

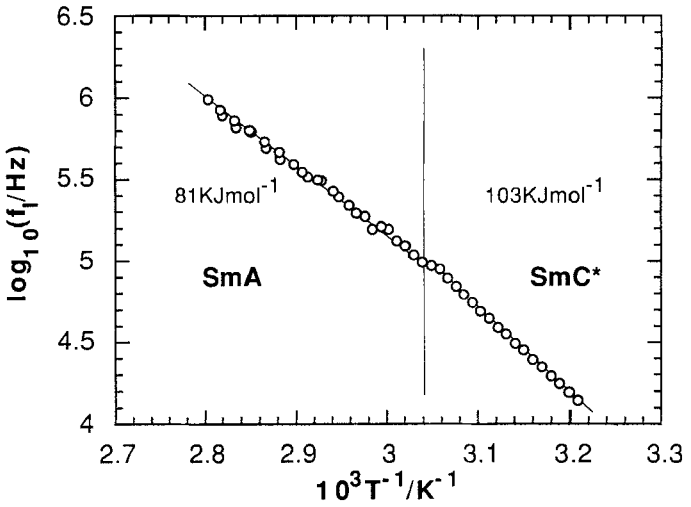

Figure 11. Arrhenius plot of the frequency of the low frequency mode.

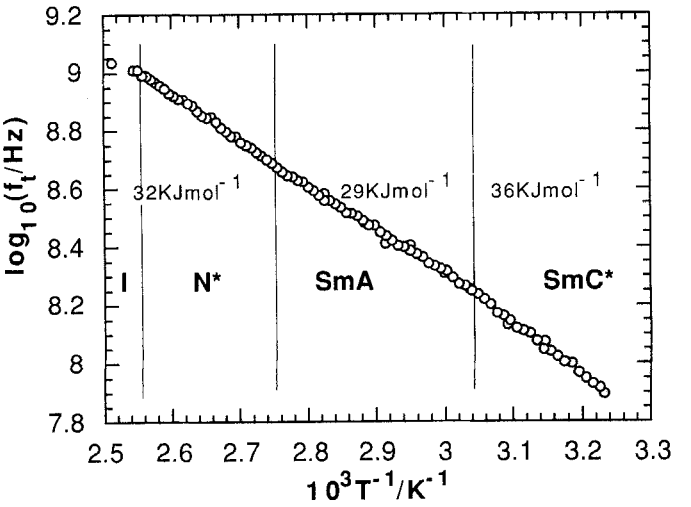

Figure 12. Arrhenius plot of the frequency of the high frequency mode.

dielectric behaviour associated with it is quite similar in chiral [18, 36] and non-chiral [30] smectogens, we could assume the above mentioned dynamics for our case. In the S_A phase, there is an isotropic distribution of identical wells, whereas in the S_C^* phase, not all the wells have the same lower level. This causes the appearance of a mean dipole moment and hence the ferroelectricity. The difference in the lower levels could be described as adding to the potential seen by the dipoles a non-chiral term proportional to the molecular tilt, similar to the one used in reference [21].

Summarizing, we have performed broad band dielectric measurements on a homeotropically aligned multicomponent mixture that exhibits N*, S_A and S_C^* phases. This study has allowed us to examine the relaxations related to rotations around the

molecular short and long axes. Neither of the two modes has jumps either in the strength or in the frequency at the S_A–S_C^* phase transition. Looking at the low frequency mode, the difference in the activation energy of its frequency could be related to a higher hindrance of the reorientation of the longitudinal dipole moment in the smectic potential in the tilted phase. For the high frequency mode, this change is smaller, indicating that the dynamics of the relaxing mechanism are basically the same in both phases. These results, together with those reported in references [17, 19, 36] for pure low molar mass and polymeric liquid crystals, allow us to conclude that this behaviour seems to be what one has to expect for all ferroelectric liquid crystals.

This work was supported by the CICYT (MAT-91-0962-C02-02) and the Universidad del País Vasco (UPV 060.310-EA049/92).

References

[1] Nordo, P. L., Rigatti, G., and Segre, U., 1973, *Molec. Phys.*, **25,** 129.
[2] Kalmykov, Y. P., 1991, *Liq. Crystals*, **10,** 519.
[3] Bata, L., and Molnar, G., 1975, *Chem. Phys. Lett.*, **33,** 535.
[4] Buka, A., and Levyraz, F., 1982, *Phys. Stat. Sol. (b)*, **112,** 289.
[5] Kresse, H., Rabenstein, P., and Demus, D., 1988, *Molec. Crystals liq. Crystals*, **154,** 1.
[6] Kresse, H., 1983, *Advances in Liquid Crystals*, Vol. 6 (Academic Press), p. 109.
[7] Bata, L., Pépy, G., and Rosta, L., 1988, *Liq. Crystals*, **3,** 893.
[8] Jadzyn, J., Parneix, J. P., Legrand, C., Njeumo, R., and Dabrowski, R., 1987, *Acta phys. pol.* A, **71,** 53.
[9] Zubia, J., Ezcurra, A., de la Fuente, M. R., Pérez Jubindo, M. A., Sierra, T., and Serrano, J. L., 1991, *Liq. Crystals*, **10,** 849.
[10] Parneix, J. P., and Legrand, C., 1988, *Ferrolectrics*, **84,** 199.
[11] Biradar, A. M., Bawa, S. S., and Chandra, S., 1992, *Phys. Rev.* A, **45,** 7282.
[12] Carlsson, T., Filipic, C., Levstik, I., snd Zeks, B., 1987, *Phys. Rev.* A, **35,** 3527.
[13] Carlsson, T., Zeks, B., Filipic, C., and Levstik, A., 1990, *Phys. Rev.* A, **42,** 877.
[14] Costello, P. G., Kalmykov, Yu. P., and Vijk, J. K., 1992, *Phys. Rev.* A, **46,** 4852.
[15] Brand, H. R., and Pleiner, H., 1991, *Phys. Rev.* A, **43,** 7063.
[16] Brand, H. R., and Pleiner, H., 1991, *Molec. Crystals liq. Crystals Lett.*, **8,** 11.
[17] Kremer, F., Schönfeld, A., Vallerien, S. U., Hofmann, A., and Schwenk, N., 1991, *Ferroelectrics*, **121,** 13.
[18] Schönfeld, A., Kremer, F., and Zentel, R., 1993, *Liq. Crystals*, **13,** 403.
[19] Kremer, F., Vallerien, S. U., Kapitza, H., Zentel, R., and Fischer, E. W., 1990, *Phys. Rev.* A, **42,** 3667.
[20] Lalanne, J. R., Buchert, C., Destrade, D., Nguyen, H. T., and Marcerou, J. P., 1989, *Phys. Rev. Lett.*, **62,** 3046.
[21] Urbanc, B., and Zeks, B., 1989, *Liq. Crystals*, **5,** 1075.
[22] Buka, A., Siemensmeyer, K., and Stegemeyer, H., 1989, *Liq. Crystals*, **6,** 701.
[23] Etxebarria, J., and Zubia, J., 1991, *Phys. Rev.* A, **44,** 6626.
[24] Zubia, J., Castro, M., Puértolas, J. A., Etxebarria, J., Pérez Jubindo, M. A., and de la Fuente, M. R., 1993, *Phys. Rev.* E, **48,** 1970.
[25] Böttcher, C. J. F., 1973, *Theory of Electric Polarization*, Vol. 1 (Elsevier), Chap. 3.
[26] Gouda, F. M., 1992, Doctoral Thesis, Chalmers University of Technology.
[27] Böttcher, C. J. F., and Bordewijk, P., 1978, *Theory of Electric Polarization*, Vol. II (Elsevier), Chap. 9.
[28] Havriliak, S., 1993, *Proceedings of the 2nd International Discussion Meeting on Relaxations in Complex Systems*, Alicante.
[29] Kresse, H., Selbmann, Ch., Demus, D., Buka, A., and Bata, L., 1981, *Cryst. Res. Technol.*, **16,** 1439.
[30] Druon, C., and Wacrenier, J. M., 1984, *Molec. Crystals liq. Crystals*, **108,** 291.
[31] Buka, A., and Bata, L., 1986, *Molec. Crystals liq. Crystals*, **135,** 49.

[32] PÉREZ JUBINDO, M. A., EZCURRA, A., DE LA FUENTE, M. R., SANTAMARIA, C., ETXEBARRIA, J., SERRANO, J. L., and MARCOS, M., 1988, *Ferroelectrics*, **89,** 587.

[33] GOODBY, J. W., 1991, *Ferroelectric Liquid Crystals*, edited by G. W. Taylor (Gordon & Breach), Chap. 2.

[34] BÖTTCHER, C. J. F., and BORDEWIJK, P., 1978, *Theory of Electric Polarization*, Vol. II (Elsevier), Chaps. 11 and 15.

[35] MARTÍNEZ, J. I., ALONSO, P. J., and ORERA, V. M., 1993, *Proceedings of the 3rd International Symposium on Metallomesogens*, Peñíscola.

[36] KREMER, F., SCHÖNFELD, A., HOFMANN, A., ZENTEL, R., and POTHS, A., 1992, *Polym. adv. Tech.*, **3,** 249.